ASEG-PESA 2015
Geophysics and Geology together for Discovery
24th International Geophysical Conference and Exhibition
15 – 18 February 2015 Perth, Western Australia

Determination of model reliability in 3-D resistivity and I.P. inversion

M.H.Loke
Geotomo Software
Penang, Malaysia
drmhloke@yahoo.com

SUMMARY

Mineral deposits frequently have complex structures that can only be resolved by 3-D inversion of resistivity and I.P. data. A nonlinear optimisation routine is commonly used to create a 3-D model from the measured apparent resistivity and I.P. data. It is particularly important to be able to assess the reliability of the anomalies seen in the inversion model before further tests are conducted. In this paper, we examine the model resolution (MR) and volume of investigation (VOI) approaches in determining model reliability. The MR method produces sections that are easier to interpret but more computationally intensive that puts practical limitations for models with more than 50000 cells. The VOI method can be used for any data set where an inversion can be carried out, but produces sections with more complex patterns and prone to local artefacts. Either method should be used for any interpretation to discern anomalies that are likely to be supported by the data.

Key words: model, reliability, resolution, VOI.

INTRODUCTION

3-D resistivity and I.P. surveys are widely used in mapping mineral deposit due to their complex nature. The resistivity model gives information about the general geology of the area, while the I.P. anomalies are more closely related to the distribution of the mineral deposits. The suspected mineral deposits are then assessed by drilling which is an expensive operation. Thus it is important to estimate the reliability of the anomalies seen in the inversion models to minimise costs.

In this paper, we examine two methods commonly used to estimate model reliability, the model resolution (MR) and volume of investigation (VOI) approaches. The following section gives brief descriptions of the nonlinear least-squares optimisation, MR and VOI methods. We then compare the results from the different methods using a field data set.

METHODS

Nonlinear least-squares optimisation method

The smoothness-constrained least-squares optimisation method is frequently used for 3-D inversion of resistivity data (Loke *et al.*, 2014b). The subsurface model consists of a large number of cells. The size and shape of the cells are fixed while the resistivity and I.P. values are varied in order to fit the observed data. The equation that gives the relationship between the model parameters and the measured data (Oldenburg and Li, 1999) is given below.

$$\left[\mathbf{J_i^T C_d J_i} + \lambda_i \mathbf{W^T C_m W}\right]\Delta\mathbf{r_i} = \mathbf{J_i^T C_d g_i} - \lambda_i \mathbf{W^T C_m W}(\mathbf{r_{i-1}} - \mathbf{r_s}) - \lambda_s(\mathbf{r_{i-1}} - \mathbf{r_s}) \quad (1)$$

The Jacobian matrix $\mathbf{J}$ contains the sensitivities of the measurements with respect to the model parameters, λ_i is the damping factor vector and $\mathbf{g_i}$ is the data misfit vector. $\mathbf{r_{i-1}}$ is the model parameter vector (the logarithm of the model resistivity values) for the previous iteration, while is $\Delta\mathbf{r_i}$ is the change in the model parameters. $\mathbf{W}$ incorporates the roughness filters in the *x*, *y* and *z* directions. $\mathbf{C_d}$ and $\mathbf{C_m}$ are weighting matrices used so that different elements of the data misfit and model roughness vectors are given equal weights if the L1-norm inversion method is used (Loke *et al.*, 2003). $\mathbf{r_s}$ is a reference model (usually a homogenous half-space). The damping factor λ_s controls the degree at which the model is constrained to be 'close' to the reference model. The finite-difference or finite-element method is used to calculate the apparent resistivity and I.P. of the inversion model. The complex resistivity method (Kenma *et al.*, 2000; Loke *et al.*, 2013) is used for I.P. models.

Model resolution

It can be shown that the model resolution matrix $\mathbf{R}$ (Loke *et al.*, 2014a) is given by

$$\mathbf{R} = \left[\mathbf{J^T C_d J} + \lambda \mathbf{W^T C_m W}\right]^{-1}\mathbf{J^T C_d J} \quad (2)$$

The main diagonal elements of $\mathbf{R}$ give an estimate of the resolution of the cells. It has a value approaching 1.0 in regions that are well constrained by the data, and 0.0 where there is no information. One problem in selecting a cut-off value to determine regions with reliable model values is that the model resolution value also depends on how finely the subsurface is subdivided into model cells. If a finer model discretization with smaller model cells is used, we would expect the resolution value for a cell at the same location will be reduced. The sum of the elements in a column of the model resolution matrix is equals to 1.0. The average value of the column elements would then be equals to *1.0/m*, where *m* is the number of model cells. To compensate for the effect of the model discretisation, we use the following index value R_c.

$$R_c(i,i)=m*R(i.i) \quad (3)$$

The spread criterion value (Oldenborger and Routh, 2009) was also calculated using off-diagonal elements of the resolution matrix, but the results are not shown as they gave results similar to the resolution plots. In this paper, direct methods are used calculate the entire resolution matrix, whereas Oldenborger and

Routh (2009) used an iterative method to calculate selected columns of the matrix. This has been made possible by advances in microcomputer technology. The PC used in this research has a hex-core CPU and 64 GB RAM. It is possible to calculate the resolution matrix for models with up to about 50000 data points or model cells within a reasonable time. However, for much larger data sets and models, it faces practical limitations.

Volume of investigation index

This technique is based on the inversion of the same data set using two widely different values of the reference resistivity (Oldenburg and Li, 1999; Oldenborger *et al.*, 2007) $\mathbf{r_s}$ in equation (1). This will produce two inversion models, $\mathbf{m_1}$ and $\mathbf{m_2}$. The volume of investigation (VOI) index is calculated using the following equation.

$$V(i,j) = \frac{m_2(i,j) - m_1(i,j)}{m_{s2} - m_{s1}} \qquad (4)$$

m_{s1} and m_{s2} are the resistivity of first and second reference models. V will approach zero where the inversion method produces the almost the same resistivity for the cell regardless of the reference model where it is well constrained by the data. In regions where the data do not have much information, V will approach a value of one as the cell resistivity will be similar to the reference resistivity. Values of greater than 0.1 are commonly used to indicate regions that are not well constrained by the data. An important advantage of the VOI method is that it can be used as long as it is possible to carry out an inversion of the data set.

RESULTS

In this section we compare plots of the MR and VOI for a survey over the Burra copper deposit in South Australia (Loke *et al.*, 2013). Figure 1 shows some of the lines from a 1966 I.P. survey using the dipole-dipole array. The data coverage is highly uneven. It has shorter lines with 50 m electrode spacing in the north and longer lines with 100 m electrode spacing in the south. The model use 50x50 m. cells, with the edges of the grid extended 200 m beyond the outermost electrodes to ensure that all regions with significant resolution are included (Loke *et al.*, 2014a). The model has 12 layers with the deepest layer set at about twice the maximum median depth of investigation (Edwards, 1977) of the arrays used. It has a total of 51168 cells. The resistivity model (Figure 2a) shows a prominent north-south low resistivity linear feature near the 1.8 km mark (x-axis) that corresponds to the Kingston Fault. The I.P. anomaly (Figure 2b) in the northern part of the fault zone corresponds to the Eagle deposit prospect. The nature of the I.P. anomaly towards the bottom-left edge of the deeper layers is uncertain as there is not much data coverage there. However it lies in the Kingston Fault zone with reports of pyrites in a nearby bore. Figure 3 show plots of the model resolution calculated using the resistivity and I.P. Jacobian matrices, and the VOI using the model resistivity values. If a cutoff value of about 50 is used for the resistivity resolution index (Figure 3a), the maximum depth of investigation is about 200 m. Not surprisingly, the highest resolution values are concentrated near the survey lines, particularly around the group of shorter spacing lines in the northern third of the survey area. This pattern is more pronounced in the I.P. resolution plots (Figure 3b). The I.P. resolution sections have a shallower maximum depth of investigation than the resistivity sections. This was confirmed by similar calculations for synthetic models with more uniform data coverage. The VOI sections give a maximum depth of investigation of about 200 m. in the southern half of the area below the longer survey lines (Figure 3c). The VOI plot show a more complex pattern with local artefacts at several places and does not always increase monotonically with depth,.

The I.P. anomaly in the northern half of the survey area lie in a region with higher resolution (and generally low VOI) values, so it is likely to be real. The southern I.P. anomaly lie in a region with low resolution (and high VOI) values, so its nature from the data alone is uncertain without independent confirmation.

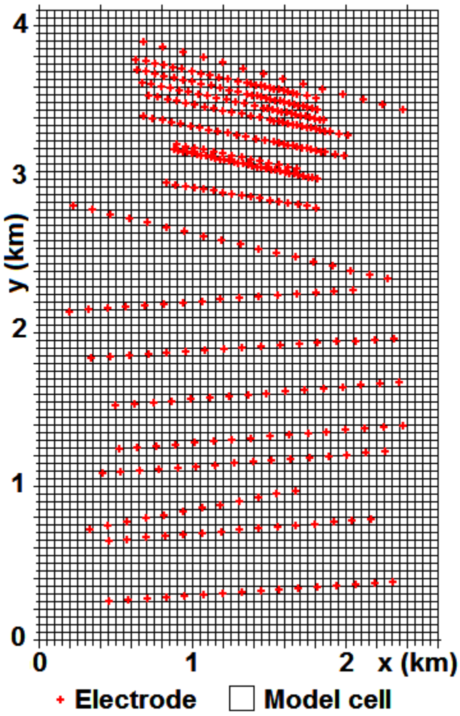

Figure 1. Burra survey electrodes and model cells layout.

CONCLUSIONS

The model resolution values are generally more robust and less affected by the particular inversion settings used, such as the L1 or L2 norms (Loke *et al.*, 2003). The VOI is less demanding computationally and can be used for problems that are too large for resolution calculations. However, it is susceptible to local artefacts and more dependent on the inversion methods used, and thus the finer features in the VOI plots should be given less weight. Either method should be used for any interpretation to discern anomalies that are likely to be supported by the data.

ACKNOWLEDGMENTS

I would like to thank Kim Frankcombe and Phoenix Copper for the Burra data set.

REFERENCES

Edwards L.S., 1977. A modified pseudosection for resistivity and induced-polarization: Geophysics, 42, 1020-1036.

Kenma, A., Binley, A., Ramirez, A. and Daily, W., 2000, Complex resistivity tomography for environmental applications: Chemical Engineering Journal, 77, 11-18.

Loke, M.H., Acworth, I., Dahlin, T., 2003, A comparison of smooth and blocky inversion methods in 2D electrical imaging surveys: Exploration Geophysics, 34 , 182-187.

Loke, M.H., Frankcoombe, K. and Rucker, D., 2013, The inversion of data from complex 3-D resistivity and I.P. surveys: ASEG-PESA 2013 23rd International Geophysical Conference and Exhibition, 11-14 August 2013 - Melbourne, Expanded Abstracts, 79.

Loke, M.H., Wilkinson, P. B., Chambers, P. B. and Strutt, M., 2014a, Optimized arrays for 2-D cross-borehole electrical tomography surveys: Geophysical Prospecting, 62, 172-189.

Loke, M.H., Dahlin, T., Rucker, D.F., 2014b, Smoothness-constrained time-lapse inversion of data from 3-D resistivity surveys: Near Surface Geophysics, 12, 5-24.

Oldenborger, G.A., Routh, P.S. and Knoll, M.D., 2007, Model reliability for 3D electrical resistivity tomography: Application of the volume of investigation index to a time-lapse monitoring experiment: Geophysics, 72, F167–F175.

Oldenborger, G.A. and Routh, P.S. 2009, The point-spread function measure of resolution for the 3-D electrical resistivity experiment: Geophysical Journal International, 176, 405-414.

Oldenburg, D.W. and Li., Y., 1999, Estimating depth of investigation in dc resistivity and IP surveys: Geophysics, 64, 403-416.

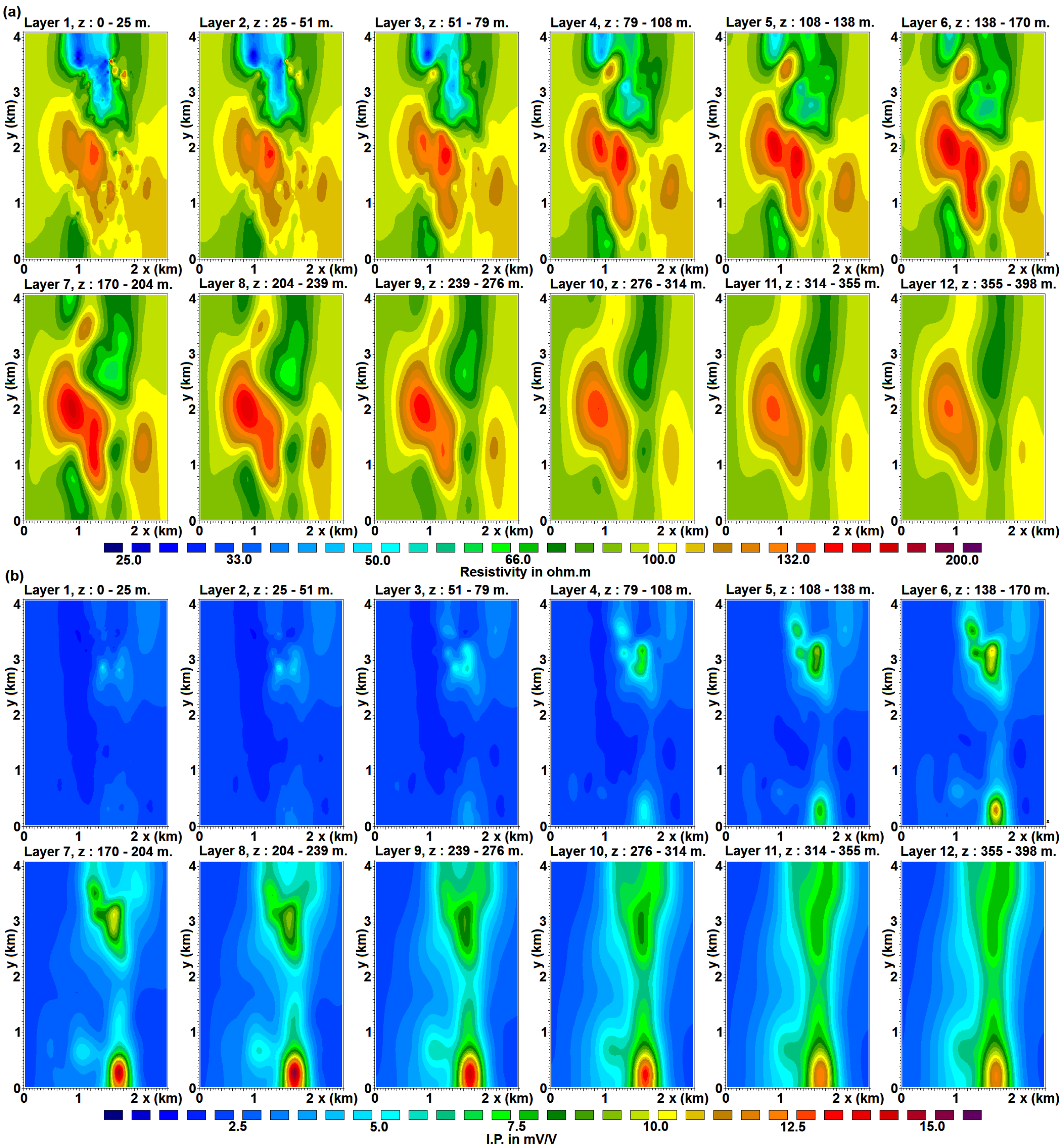

Figure 2. Burra survey (a) resistivity and (b) I.P. inversion model layers.

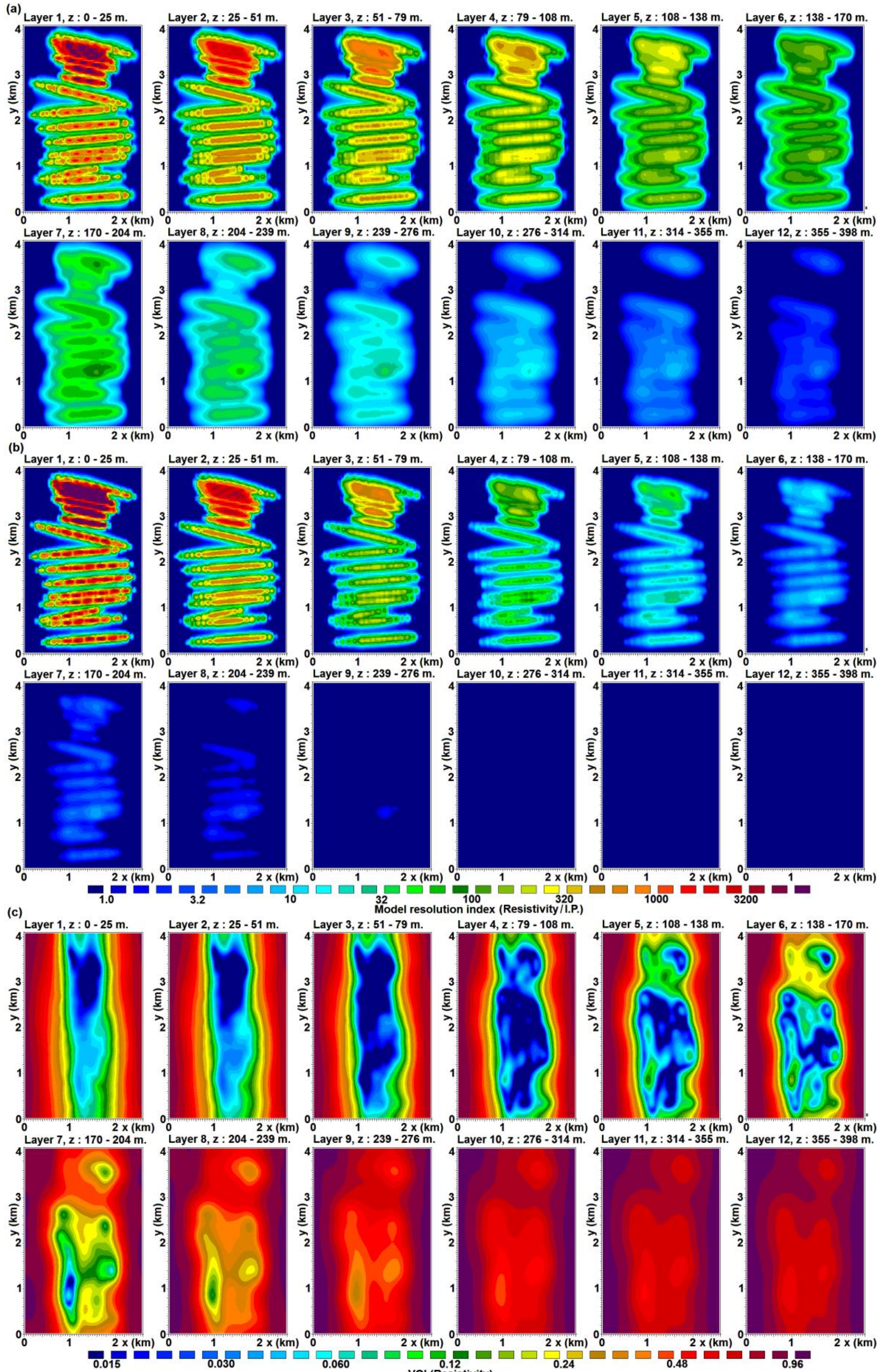

Figure 3. The model (a) resistivity and (b) I.P. resolution index, and (c) VOI values.